

Slow, bursty dynamics as a consequence of quenched network topologies

Géza Ódor

Research Center for Natural Sciences, Hungarian Academy of Sciences, MTA TTK MFA, P.O. Box 49, H-1525 Budapest, Hungary

(Received 27 January 2014; published 2 April 2014)

Bursty dynamics of agents is shown to appear at criticality or in extended Griffiths phases, even in case of Poisson processes. I provide numerical evidence for a power-law type of intercommunication time distributions by simulating the contact process and the susceptible-infected-susceptible model. This observation suggests that in the case of nonstationary bursty systems, the observed non-Poissonian behavior can emerge as a consequence of an underlying hidden Poissonian network process, which is either critical or exhibits strong rare-region effects. On the contrary, in time-varying networks, rare-region effects do not cause deviation from the mean-field behavior, and heterogeneity-induced burstiness is absent.

DOI: [10.1103/PhysRevE.89.042102](https://doi.org/10.1103/PhysRevE.89.042102)

PACS number(s): 05.70.Ln, 89.75.Hc, 89.75.Fb

I. INTRODUCTION

The dynamics of systems with general network communications has been an interesting topic of various models and empirical observations [1,2]. In networks with large topological dimension defined as $N \propto r^D$, where N is the number of nodes within the (chemical) distance r , the evolution is expected to be exponentially fast. A generic, slow power-law type of dynamics is reported in [3–8]. In social and neural networks, the occurrence of generic slow dynamics was suggested to be the result of non-Poissonian, bursty behavior of agents [9] connected by small-world networks [6,10–12]. Times between contacts [13] or communication [14,15] between individuals was found to deviate from a Poisson process, namely an intermittent switching between periods of low activity and high activity, resulting in fat-tailed intercommunication time distributions [16].

On the other hand, arbitrarily large rare regions (RRs) that can change their state exponentially slowly as a function of their sizes can cause the so called Griffiths phase (GP) [17,18], in which slow, nonuniversal power-law dynamics occurs [19]. It has been shown [19–21] that GPs can emerge as a consequence of purely topological disorder. However, this has been found only in finite-dimensional networks, or in weighted treelike networks for an extended time window [22–24].

Griffiths singularities affect the dynamical behavior both below and above the transition point and can best be described via renormalization-group methods in networks [25–27]. GPs were shown by optimal fluctuation theory and simulations of the contact process (CP) [28,29] on Erdős-Rényi (ER) networks [30] and on generalized small-world (GSW) networks [31–33].

The susceptible-infected-susceptible (SIS) model [34] is another fundamental system to describe simple epidemic (information) -possessing binary site variables: infected (active) or healthy (inactive). Infected sites propagate all of their neighbors the epidemic (or the activation) with rate λ or recover (spontaneously deactivate) with rate 1. SIS differs from the CP in which the branching rate is normalized by k , the number of outgoing edges of a vertex, thus it allows an analytic treatment using symmetric matrices. By decreasing the infection (communication) rate of the neighbors, a continuous phase transition occurs at some λ_c critical point from a steady state

with finite activity density ρ to an inactive one, with $\rho = 0$ (see [35–37]). The latter is also called absorbing, since no spontaneous activation of sites is allowed.

Very recently it has been proposed [38] that many networks cannot be considered quenched, but they evolve on the same time scale as the dynamical process running on top of them. Activity-driven network models have been introduced in which at a given time, nodes possess only a small number ($m = 2$) of edges selected via a fixed, node-dependent activity potential V_i , which exhibits the probability distribution $F(V) \propto V^{-\gamma}$. Asymptotically, the integrated link distribution is shown to be a scale-free (SF) network with $P(k) \propto k^{-\gamma}$ degree distribution [38]. In this work, I performed extensive numerical simulations to investigate whether rare-region effects and bursty dynamics could be observed in such networks with CP or annihilating-random-walk (ARW) (see [36]) processes running on them.

II. BURSTINESS IN THE CRITICAL CONTACT PROCESS

The one-dimensional (1D) critical CP was simulated on rings of size $N = 10^5$. The system was started from a fully occupied state up to $t = 10^6$ Monte Carlo steps (MCSs) (throughout this paper, time is measured in MCSs and shown to be unitless in the figures). MCSs are built up from full sweeps of active sites. In one elementary MCS, an active site is selected randomly and the activation is removed with probability $1 - p = 1/(1 + \lambda)$. Alternatively, one of its randomly selected neighbors is activated with probability $p = \lambda/(1 + \lambda)$. The simulations were done around the critical point $\lambda_c = 3.29785$ [39] of the CP. During the simulations, the times and the intercommunication times (Δ) of neighbor activations of sites are calculated and histogrammed. Following the repetition of ~ 200 independent runs, these timing data were analyzed and the probability distribution $P(\Delta)$ is calculated (see Fig. 1).

The systems during the runs are in a nonstationary state, hence the average Δ should increase as it approaches extinction. Still, $P(\Delta)$ for finite sizes exhibits a power-law tail, characterized by $P(\Delta) \sim \Delta^{-x}$ with the exponent $x = 1.85(5)$, obtained by least-squares fitting to the data. To check if the nonstationary state would cause a change in $P(\Delta)$, the histogramming was performed for the early ($t \leq 5 \times 10^5$ MCSs) and late ($t > 5 \times 10^5$ MCSs) events separately. One cannot see any differences, as all three $P(\Delta)$ distributions

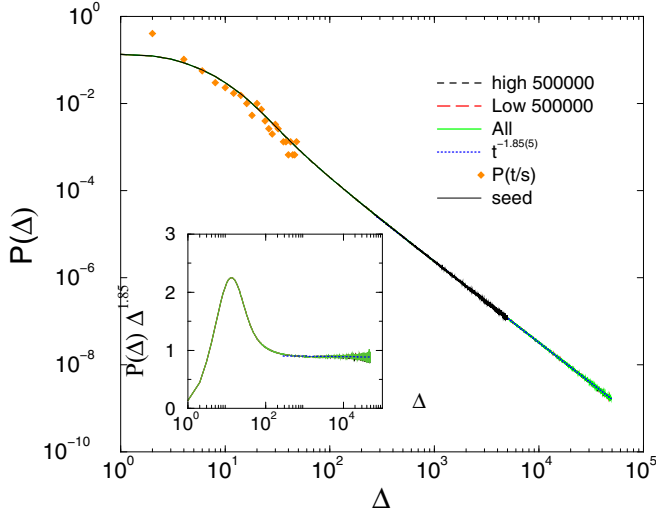


FIG. 1. (Color online) Intercommunication time distribution in the 1D critical CP of size $N = 10^5$. The full line denote histogramming from all times, the dashed line from high times, and long dashes from low times. The dotted line shows a power-law fit for $t > 200$ resulting in $\propto t^{-1.85(5)}$. The solid thin line corresponds to runs from seed initial conditions. Inset: the same data multiplied by the $t^{1.85}$ corresponding to the tail decay.

exhibit power-law behavior. On the other hand, the $P(\Delta)$ distributions above or below λ_c show exponential tails, as expected.

The scaling behavior at the critical point can be derived by expressing the intercommunication probability via the temporal autocorrelation function. Infection events can happen if there is an infected-uninfected neighbor pair, a kink in the spin language: $n_i(t) = 1$, at site i and time t . Using the two-time autocorrelation function $\Gamma(t, s)$, one can estimate the probability of the subsequent infection events, separated by a communication-free period Δ as

$$P(\Delta) \simeq p^2 \Gamma(t, s) \prod_{j=1}^{j < \Delta} \{(1-p)\Gamma(j, s) + [1 - \Gamma(j, s)]\} \simeq \Gamma(t, s) \quad (1)$$

using the connected temporal correlator between times s and t ,

$$\Gamma(t, s) = \langle n_i(t)n_i(s) \rangle - \langle n_i(t) \rangle \langle n_i(s) \rangle. \quad (2)$$

Here $\langle \rangle$ denotes averaging for independent runs. In this estimate, the correlations among the intercommunication time events are neglected; however, this does not affect the asymptotic behavior, because terms in the product are $\simeq O(1)$.

For 1D CP it is well known that this function exhibits an aging behavior (see [37,40]), i.e., time translational invariance is broken, but in the $t, s \rightarrow \infty$ limit the densities $\langle n_i(t) \rangle \rightarrow 0$ and the correlator scales as

$$\Gamma(t, s) \propto (t/s)^{-\theta} = (\Delta/s + 1)^{-\theta}. \quad (3)$$

In the case of 1DCP, $\theta = 1.80(5)$ (see [37,40]). This is also true for the kink variables, which also follow the same universal scaling behavior, belonging to the directed percolation class

[37]. Strictly speaking, due to the aging behavior we have the scale dependence $P(t/s) \sim \Delta^{-\theta}$ and indeed the simulations confirm this (see Fig. 1). Asymptotically, one can find the same leading-order contribution for $P(\Delta)$, coming from the smallest s in the statistical average, and the tail behaviors agree with the autocorrelation function decay.

More generally, the site occupancy restriction condition of the CP is not a necessary condition to find fat intercommunication tails. One can easily deduce that the power-law tail of $\Gamma(t, s)$ of infections causes also fat tails of the link-activation intercommunication times. This has been confirmed by the simulations. Furthermore, simulation runs that started from small activated seeds (see [37]) resulted in the same tail in $P(\Delta)$ again (see Fig. 1), only the distribution of activation times changed. Contrary to the full initial condition case, in which it decays as $\sim \Delta^{-0.16(1)}$, it increases as $\sim \Delta^{0.33(1)}$ in the case of seeds.

III. BURSTYNESS OF THE CP ON GENERALIZED SMALL-WORLD NETWORKS

In this section, I present results obtained for the CP on certain GSW networks [41]. It has been shown that these system exhibit extended GP regions, with nonuniversal, λ -dependent power-law dynamics [19,21]. The network generation starts with N nodes on a ring. All nearest neighbors are connected with Euclidean distance $l = 1$ with probability 1 and pairs with $l > 1$ with a probability $p(l) = 1 - \exp(-\beta l^{-s})$. For a large distance, this results in $p(l) \simeq \beta l^{-s}$. Now I consider the following cases: $s = 2$ with $\beta = 0.1$ and 0.2 .

The intercommunication times of nodes were followed in networks with $L = 10^6$ nodes up to $t_{\max} = 10^6$ MCSs, as in case of the pure CP. The number of independent samples at a given parameter, for which averaging was done, varied between 200 and 1000. The $P(\Delta)$ distributions were determined for several λ 's in the GP of these networks. Invariance of $P(\Delta)$ with respect to the measuring time windows has been checked, similarly to the pure critical CP case.

As Fig. 2 shows, power-law tails emerge again, with slightly λ -dependent slopes for $\beta = 0.1$ at $\lambda = 2.97, 3.02, 3.07$ within the GP region of the model. To see the dependency on λ and the corrections to scaling, I applied the standard local slope analysis (see [37]) on the $P(\Delta)$ results. The effective exponent of x , calculated as the discretized logarithmic derivative

$$x_{\text{eff}}(t) = \frac{\ln P(\Delta') - \ln P(\Delta)}{\ln(\Delta) - \ln(\Delta')}, \quad (4)$$

where $\Delta/\Delta' = 2$. As one can see from the inset of Fig. 2, at the critical point $\lambda_c = 3.07(1)$, determined in [21], x tends to $1.90(1)$ asymptotically as $\Delta \rightarrow \infty$. Below λ_c , the effective exponents converge to smaller values: $x = 1.92(1)$ at $\lambda = 3.02$ and $x = 1.96(1)$ at $\lambda = 2.97$. Corrections to the scaling are rather strong for $\Delta < 5000$, but the effective exponents seem to saturate asymptotically. Note that, as in case of the density decay study of this model [21], logarithmic corrections were found in the GP.

As in case of the 1D CP, the tail results are not affected by using an active initial seed condition or by measuring the times between the communication attempts of the sites. The

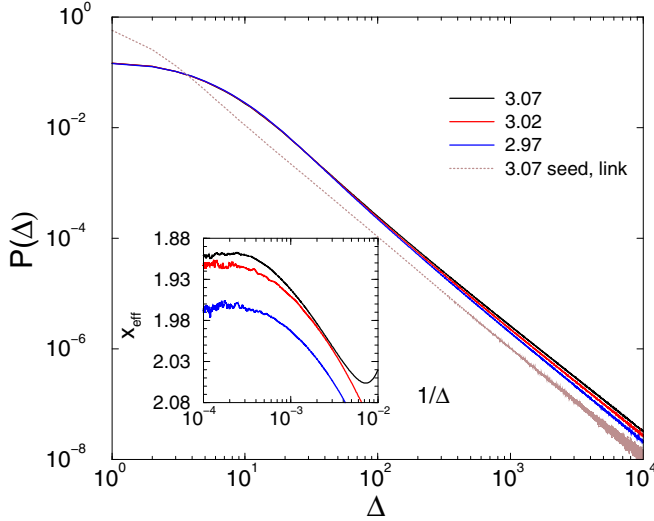


FIG. 2. (Color online) Intercommunication time distribution in the GP of a GSW network with $\beta = 0.1$ of size $N = 10^6$ and $\lambda = 2.97, 3.02, 3.07$ (bottom to top solid curves). The solid thin line corresponds to runs from seed initial conditions measuring all activation attempts. Inset: effective exponents defined as (4) of the same data.

combined effect of these two modifications is shown in Fig. 2 for $\lambda_c = 3.07$.

For $\beta = 0.2$, one finds somewhat different power-law tails inside the GP (see Fig. 3). The local slope analysis suggests $x = 1.94(1)$ at $\lambda_c = 2.85$, $x = 1.96(1)$ at $\lambda = 2.8$, and $x = 1.99(1)$ at $\lambda = 2.75$. One can clearly see tail behaviors, characterized by increasing x exponents with β , in agreement with the fact that the addition of long edges to the network increases the topological dimension, thus the autocorrelation exponent, which is $\theta = 4$ in the mean-field limit.

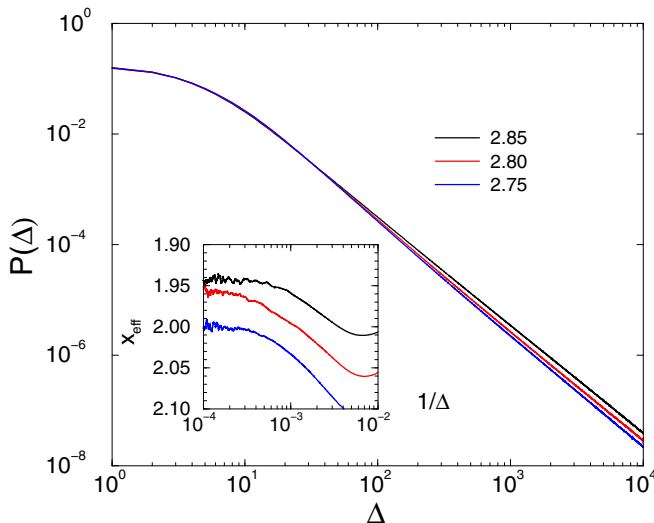


FIG. 3. (Color online) Intercommunication time distribution in the GP of a GSW network with $\beta = 0.2$ of size $N = 10^6$ and $\lambda = 2.75, 2.8, 2.85$ (bottom to top curves). Inset: effective exponents defined as (4) of the same data.

IV. BURSTYNESS OF THE SIS MODEL ON AGING SF NETWORKS

In this section, I present the SIS model results on aging SF networks, where cutting the links among highly connected nodes results in finite topological dimension and GP behavior [24]. In the original Barabási-Albert (BA) [42] graph construction, one starts with a single connected node and adds new links following the linear preferential rule. In [24], I investigated a generalized model in which a fraction of the edges of the aging nodes was removed from the BA graph by following a random, linear preferential rule. Consequently, the edge distribution of the BA graph, $P(k) \propto k^{-3}$, was cut off by an exponential factor for large k 's, and quenched mean-field theory suggested a GP behavior in agreement with the dynamical simulations.

SIS model density simulations were run on systems with $N = 10^5$ nodes in the formerly determined GP region $2.4 < \lambda < 2.7$ of the aging BA graphs [24]. The occurrence of fat tail $P(\Delta)$ distributions can be seen in Fig. 4, but now an even network site (i) dependency emerges. This is related to the fact that nodes are inhomogeneous: the average number of edges decreases as $\langle k_i \rangle \sim i^{-1/2}$ by the BA network generation. Least-squares error power-law fitting for $\Delta > 20$ leads to λ and i dependent decay exponents. For $\lambda = 2.65$ and $i = 1$ (highest connectivity node), the $P(\Delta)$ decay is characterized by the exponent $x = 3.48(3)$, which is near the mean-field value of the autocorrelation: $\theta = 4$ of the CP. For less connected nodes ($i = 100$), the decay is slower: $P(\Delta) \propto \Delta^{-2.96(3)}$, getting away from the mean-field value and coming closer to the one-dimensional autocorrelation exponent of CP. This agrees with our expectations, since for larger i 's the connectivity decreases and the system exhibits autocorrelations of lower dimensionality. By decreasing λ in the GP, as shown in Fig. 4, we obtain the following decreasing series of asymptotic tail

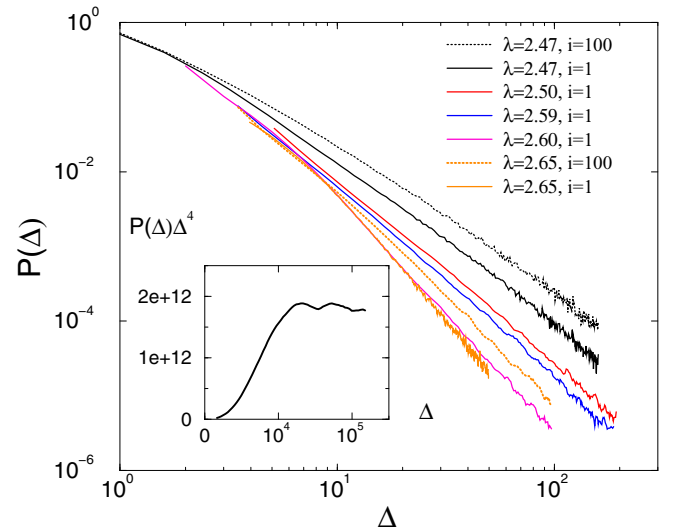


FIG. 4. (Color online) Intercommunication time distribution in the GP of an aging BA network of size $N = 10^5$ for $\lambda = 2.47, 2.5, 2.55, 2.59, 2.6, 2.65$ (top to bottom curves) and measured at different ($i = 1$ and 100) sites. Power-law fitting exponents for the tail behavior are shown in the text. Inset: $P(\Delta)\Delta^4$ at the λ_c of the CP defined on the pure BA graph.

exponents for $i = 1$: $x = 3.48(3)$, $3.12(3)$, $2.64(2)$, $2.52(25)$, $2.42(2)$. For $i = 100$ at $\lambda = 2.47$, the tail exponent is $x = 2.13(2)$. Again, logarithmic corrections to the dynamic scaling can also be expected in the GP [18].

To complete this study, I also tested the critical point behavior of $P(\Delta)$ in the case of CP on the pure BA network (see [22]) at $\lambda_c = 1.21$. As the inset of Fig. 4 shows, the tail behavior tends to a power law with $x = 4$ for $\Delta > 20.000$.

V. DYNAMICS OF THE CP AND ARW ON TIME-VARYING NETWORKS

A simulation program has been created with a fixed activity potential $F(V) \propto V^{-\gamma}$ attached to vertexes, such that two edges are connected to each node with that probability before each “sweep” of the network. One sweep (or Monte Carlo step) consists of N random CP updates of the network of N nodes. I followed $\rho(t)$ after starting from a fully occupied (infected) state. The time is updated by one MCS after a full network sweep. The simulations were run up to $t_{\max} = 2 \times 10^5$ MCSs on several sizes up to $N = 10^7$ and repeated for 10^2 – 10^3 independent randomly generated networks.

First a $\gamma = 3$ type of network has been studied. The finite-size effects are strong, but for large sizes ($N \sim 10^7$) a phase transition seems to appear with $\rho \propto 1/t$ decay, which agrees with the heterogeneous mean-field prediction [22] (see Fig. 5). Similar results have been found for $\gamma = 2.8$ networks.

I have also tested the dynamical behavior of the annihilating random walk (ARW) [37] in networks with activity potential parameters: $\gamma = 0.6, 0.8, 0.9, 1, 3.8$. The ARW model is a solvable model in homogeneous, Euclidean system, in which randomly selected particles hop to neighboring empty sites or annihilate with others upon collision. In the high-dimensional mean-field limit, the density of particles decays asymptotically as $t \propto 1/t$. As Fig. 6 shows, simulations up to $t_{\max} = 10^5$ MCSs with $N = 10^7$ nodes result in the same asymptotic

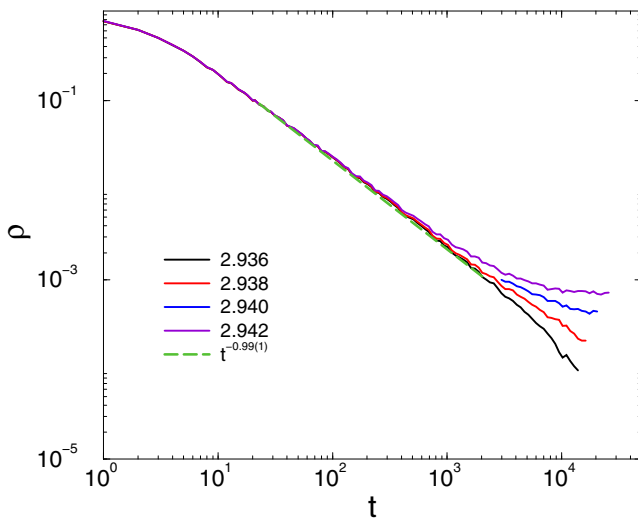


FIG. 5. (Color online) Density decay of the contact process in time-varying networks of sizes $N = 10^7$ for $\lambda = 2.936, 2.938, 2.940, 2.942$ (bottom to top). The dashed line shows a power-law fit to the $\lambda = 2.94$ (critical) curve. The activity potential decays with $\gamma = 3$.

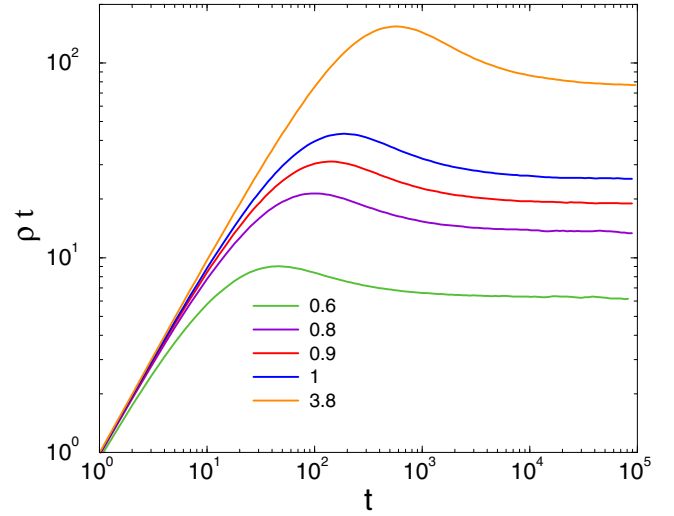


FIG. 6. (Color online) Density decay in the ARW in time-varying networks of sizes $N = 10^7$ for $\gamma = 0.6, 0.8, 0.9, 1, 3.8$ (bottom to top). The curves are the average of 10^3 independent runs.

mean-field behavior following a long crossover time. This suggests that slow, nonuniversal dynamics in activity-driven time-varying networks does not exist, strengthening the hypothesis [20] that quenched heterogeneity is a necessary condition for observing rare-region effects.

Not so surprisingly, burstyness does not occur in such time-varying networks either, because the network rewiring process destroys the long-range dynamical correlations. Simulations result in exponential tail $P(\Delta)$ distributions.

VI. CONCLUSIONS

The observed burstyness in network systems is assumed to be related to the internal, non-Poissonian behavior of agents or state variables. This has been explained by different multilevel or time-scheduling internal models. In this paper, I demonstrated an alternative route to this, being a natural consequence of correlated, complex behavior of the whole system. In the case of the critical, one-dimensional contact process, fat-tailed intercommunication time distribution arises related to the diverging autocorrelation function. Furthermore, with the addition of long edges, which turns the network into GSWs with Griffiths phases, one can observe topology-dependent, fat-tailed intercommunication time distributions.

I have also shown that in the case of an aging scale-free network that exhibits Griffiths phase, these power-law distributions depend also on the average connectivity of nodes. The observed tail exponents vary in the range $x = 2$ – 4 , which is smaller than the experimental values reported in human communication data sets [10,11]. However, as the GSW model example shows, there are networks that possess smaller topological dimensions, where $x < 2$. Furthermore, there are other models [40], such as the bosonic contact process or the bosonic pair contact process, where the autocorrelation decays slower ($\theta = D/2$ for these unrestricted CPs [43]), thus x could also be smaller in networks.

It is important to note that these systems are in a nonstationary state during the simulations while the tail distributions

remain time-invariant and initial condition invariant. Usually real systems are also in a nonstationary state as a consequence of various external conditions, such as circadian oscillations. In the case of regular networks, the distributions are site-invariant as well.

Finally, I have shown that both the contact process and annihilating random walks exhibit mean-field-like dynamics in time-varying, scale-free networks in which GP effects are absent and the distribution of intercommunication times is not bursty, but is characterized by an exponential tail distribution.

These results suggest that bursty behavior can emerge as a collective behavior in quenched network systems close to criticality or in extended GP-like regions, suggesting the

necessity for a closer inspection of such systems. When real-world data confirm that sites exhibit inherent bursty behavior, the overlap of the two reasons should emerge, possibly with the outcome of the more relevant one, which decays more slowly.

ACKNOWLEDGMENTS

I thank R. Juhász, J. Kertész, F. Iglói, and R. Pastor-Satorras for their useful comments. Support from the Hungarian research fund OTKA (Grant No. K109577), HPC-EUROPA2 pr.228398, and the European Social Fund through project FuturICT.hu (Grant No. TAMOP-4.2.2.C-11/1/KONV-2012-0013) is acknowledged.

-
- [1] S. N. Dorogovtsev, A. V. Goltsev, and J. F. F. Mendes, *Rev. Mod. Phys.* **80**, 1275 (2008).
- [2] A. Barrat, M. Barthélemy, and A. Vespignani, *Dynamical Processes on Complex Networks* (Cambridge University Press, Cambridge, 2008).
- [3] S. Johnson, J. J. Torres, and J. Marro, *PLoS ONE* **8**, e50276 (2013).
- [4] R. Pastor-Satorras and A. Vespignani, *Phys. Rev. Lett.* **86**, 3200 (2001).
- [5] R. Pastor-Satorras and A. Vespignani, *Evolution and Structure of the Internet: A Statistical Physics Approach* (Cambridge University Press, Cambridge, 2004).
- [6] M. Karsai, M. Kivela, R. K. Pan, K. Kaski, J. Kertész, A.-L. Barabási, and J. Saramäki, *Phys. Rev. E* **83**, 025102(R) (2011).
- [7] A. Haimovici, E. Tagliazucchi, P. Balenzuela, and D. R. Chialvo, *Phys. Rev. Lett.* **110**, 178101 (2013).
- [8] P. Moretti and M. Muñoz, *Nat. Commun.* **4**, 2521 (2013).
- [9] A.-L. Barabasi, *Bursts* (Dutton, New York, 2010).
- [10] M. Karsai, K. Kaski, A.-L. Barabási, and J. Kertész, *Sci. Rep.* **2**, 397 (2012).
- [11] M. Karsai, K. Kaski, and J. Kertész, *PLoS ONE* **7**, e40612 (2012).
- [12] R. Lambiotte, L. Tabourier, and J.-C. Delvenne, *Eur. Phys. J. B* **86**, 320 (2013).
- [13] C. Cattuto, W. V. den Broeck, A. Barrat, V. Colizza, J.-F. Pinton, and A. Vespignani, *PLoS ONE* **5**, e11596 (2010).
- [14] J. Kleinberg, *Data Mining Knowledge Discovery* **7**, 373 (2003).
- [15] J.-P. Eckmann, E. Moses, and D. Sergi, *Proc. Natl. Acad. Sci. USA* **101**, 14333 (2004).
- [16] A.-L. Barabasi, *Nature (London)* **435**, 207 (2005).
- [17] R. B. Griffiths, *Phys. Rev. Lett.* **23**, 17 (1969).
- [18] T. Vojta, *J. Phys. A* **39**, R143 (2006).
- [19] M. A. Muñoz, R. Juhász, C. Castellano, and G. Ódor, *Phys. Rev. Lett.* **105**, 128701 (2010).
- [20] G. Ódor, R. Juhász, C. Castellano, and M. A. Muñoz, in *Nonequilibrium Statistical Physics Today*, edited by P. L. Garrido, J. Marro, and F. de los Santos (AIP, New York, 2011), Vol. 1332, pp. 172–178.
- [21] R. Juhász, G. Ódor, C. Castellano, and M. A. Muñoz, *Phys. Rev. E* **85**, 066125 (2012).
- [22] G. Ódor and R. Pastor-Satorras, *Phys. Rev. E* **86**, 026117 (2012).
- [23] G. Ódor, *Phys. Rev. E* **87**, 042132 (2013).
- [24] G. Ódor, *Phys. Rev. E* **88**, 032109 (2013).
- [25] C. Monthus and T. Garel, *J. Phys. A* **44**, 085001 (2011).
- [26] I. A. Kovács and F. Iglói, *J. Phys.: Condens. Matter* **23**, 404204 (2011).
- [27] R. Juhász and I. A. Kovács, *J. Stat. Mech.* (2013) P06003.
- [28] T. E. Harris, *Ann. Prob.* **2**, 969 (1974).
- [29] T. M. Liggett, *Interacting Particle Systems* (Springer-Verlag, New York, 1985).
- [30] P. Erdős and A. Rényi, *Publ. Math.* **6**, 290 (1959).
- [31] M. Aizenman and C. M. Newman, *Commun. Math. Phys.* **107**, 611 (1986).
- [32] R. Juhász, *Phys. Rev. E* **78**, 066106 (2008).
- [33] R. Juhász and G. Ódor, *Phys. Rev. E* **80**, 041123 (2009).
- [34] R. M. Anderson and R. M. May, *Infectious Diseases in Humans* (Oxford University Press, Oxford, 1992).
- [35] J. Marro and R. Dickman, *Nonequilibrium Phase Transitions in Lattice Models* (Cambridge University Press, Cambridge, 1999).
- [36] G. Ódor, *Rev. Mod. Phys.* **76**, 663 (2004).
- [37] G. Ódor, *Universality in Nonequilibrium Lattice Systems* (World Scientific, Singapore, 2008).
- [38] N. Perra, B. Goncalves, R. Pastor-Satorras, and A. Vespignani, *Sci. Rep.* **2**, 469 (2012).
- [39] M. Henkel, H. Hinrichsen, and S. Lübeck, *Non-Equilibrium Phase Transitions* (Springer, New York, 2008), Vol. 1.
- [40] M. Henkel and M. Pleimling, *Non-equilibrium Phase Transitions, Vol. 2: Ageing and Dynamical Scaling Far from Equilibrium* (Springer, Heidelberg, 2010).
- [41] I. Benjamini and N. Berger, *Rand. Struct. Alg.* **19**, 102 (2001).
- [42] A.-L. Barabási and R. Albert, *Science* **286**, 509 (1999).
- [43] F. Baumann, S. Stoimenov, and M. Henkel, *J. Phys. A* **39**, 4095 (2006).